Magnitude distribution complexity revealed in seismicity from Greece

Stanislaw Lasocki[1] and Eleftheria E. Papadimitriou[2]

Received 25 April 2005; revised 29 April 2006; accepted 29 August 2006; published 28 November 2006.

[1] The structure of the magnitude distribution of earthquakes from three different seismotectonically homogeneous areas of Greece has been investigated by means of statistical inference methods. Unlike in previous studies, a nonparametric approach, namely, the smoothed bootstrap test for multimodality applied in this work makes it possible to test the complexity of the distribution without specifying any particular probabilistic model. Two null hypotheses, the number of modes in magnitude density equals 1 and the number of bumps in magnitude density equals 1, have been considered. Their alternatives mean that the magnitude population has a multicomponent structure. In two out of three studied cases the significance of the null hypotheses is less than 10%, which indicates that the magnitude distribution follows neither the log linear nor any smoothly non–log linear law but is more complex. Consequently, when the log linear model is applied to represent the magnitude distribution of each of the cases studied, estimates of mean return periods dramatically disagree with earthquake recurrence observations. The most significant differences are for large magnitude range; that is, such return period estimates are the most erroneous for large earthquakes. It has also been shown that the hazard estimation can be improved considerably by using the model-free approach with the kernel estimator of magnitude density. This approach ensures a satisfactory agreement between the mean return period estimates and actual observations, and in most of the cases, the agreement is very good.

Citation: Lasocki, S., and E. E. Papadimitriou (2006), Magnitude distribution complexity revealed in seismicity from Greece, *J. Geophys. Res.*, *111*, B11309, doi:10.1029/2005JB003794.

1. Introduction

[2] In recent years several authors have indicated that there are breaks in scaling in frequency-magnitude distribution or, more generally, that the distribution for worldwide data, as well as regional earthquake data, does not follow the log linear Gutenberg-Richter law but is more complex [e.g., *Wesnousky et al.*, 1983; *Davison and Scholz*, 1985; *Pacheco and Sykes*, 1992; *Stirling et al.*, 1996; *Knopoff*, 2000; *Leonard et al.*, 2001]. Others, however, have expressed doubts in this regard [e.g., *Kagan*, 1993, 1996, 1999; *Sornette et al.*, 1996; *Sornette and Sornette*, 1999; *Main*, 2000]. Doubtlessly, the question on the actual shape of the magnitude distribution is not trivial and cannot be readily answered. Earthquake catalogs are dominated by smaller events. Nonlinear features of the distribution are often expected at larger magnitudes [e.g., *Pacheco et al.*, 1992; *Aki*, 2000; *Stock and Smith*, 2000]; hence if they exist, they concern a small percentage of the sample and can be effectively obscured. Moreover, statistical inference methods, which have been so far applied to investigate complexity in the magnitude-frequency relationship, are most commonly used to test the appropriateness of an assumed complex model of magnitude distribution. Such methods, however, cannot yield unquestionable conclusions because goodness of fit testing procedures provide strong indications on the low, but not on the high significance of the null hypotheses.

[3] A smoothed bootstrap test for multimodality [*Silverman*, 1986; *Efron and Tibshirani*, 1993] offers a new way of dealing with the problem. In this nonparametric test, earthquake data can be investigated under the null hypotheses, which state that the magnitude distribution is not complex, without specifying any particular model of the distribution either for the null or for the alternative hypotheses. The first applications of this novel approach to induced seismicity data [*Lasocki*, 2001] as well as worldwide and regional earthquake data [*Lasocki*, 2002] provided distinct indications of the complex structure of the magnitude distribution. In the current work, we present some modifications of the testing procedure, which make it more effective within the problem area, the results of magnitude complexity studies for regional earthquake data from Greece and the implication of the uncovered complexity of magnitude distribution for probabilistic seismic hazard analysis.

2. Method of Analysis

2.1. Null Hypotheses

[4] In an extensive review, *Utsu* [1999] discussed several recently used magnitude distribution models. With the one

[1]Faculty of Geology, Geophysics and Environmental Protection, AGH University of Science and Technology, Krakow, Poland.
[2]Geophysics Department, School of Geology, Aristotle University of Thessaloniki, Thessaloniki, Greece.

0148-0227/06/2005JB003794$09.00

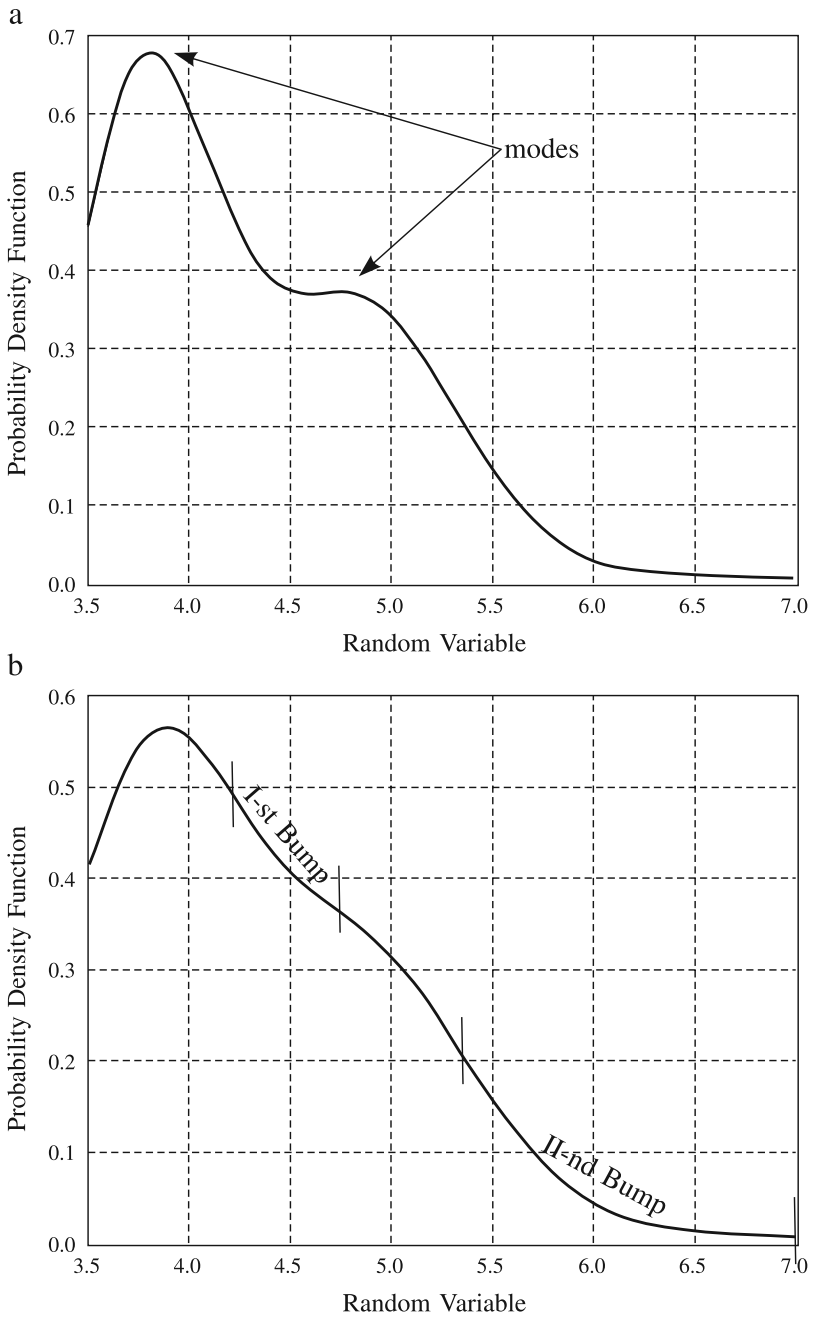

Figure 1. Examples of complex exponential-like distributions. (a) A bimodal probability density function. (b) A two-bump density function.

exception of the bilinear model, all the models have one feature in common: the logarithm of their probability density of magnitude is either linear or smoothly nonlinear. The distributions with log linear density directly result from the Gutenberg-Richter's recurrence relation and are truncated exponential distributions e.g., the left-hand side truncated exponential [*Aki*, 1965] and doubly truncated exponential [*Cosentino et al.*, 1977] distributions. The smooth nonlinearity of the logarithmized magnitude density means that the density has, at most, one local maximum (mode) and one inflexion point to the right of the mode. The most popular examples of the smoothly non–log linear models include the tapered Gutenberg-Richter [*Jackson and Kagan*, 1999] and Weibull [*Lasocki*, 1993] distributions for magnitude and the gamma [*Kagan*, 1999] and the generalized Pareto [*Pisarenko and Sornette*, 2003] distributions for the seismic moment. All magnitude distributions that lead to a self-similarity of seismic moment and seismic energy are either log linear or smoothly non–log linear distributions.

[5] As opposed to the log linear and smoothly non–log linear distributions above, more complex distributions are represented by densities that have more than one mode and/or more than one bump to the right of the global maximum. A mode is a local maximum of probability density and a bump is an interval $[a, b]$ such that the probability density is concave over $[a, b]$ but not over any larger interval [*Silverman*, 1986]. Examples of the bimodal and two bump probability density functions are shown in Figure 1. The

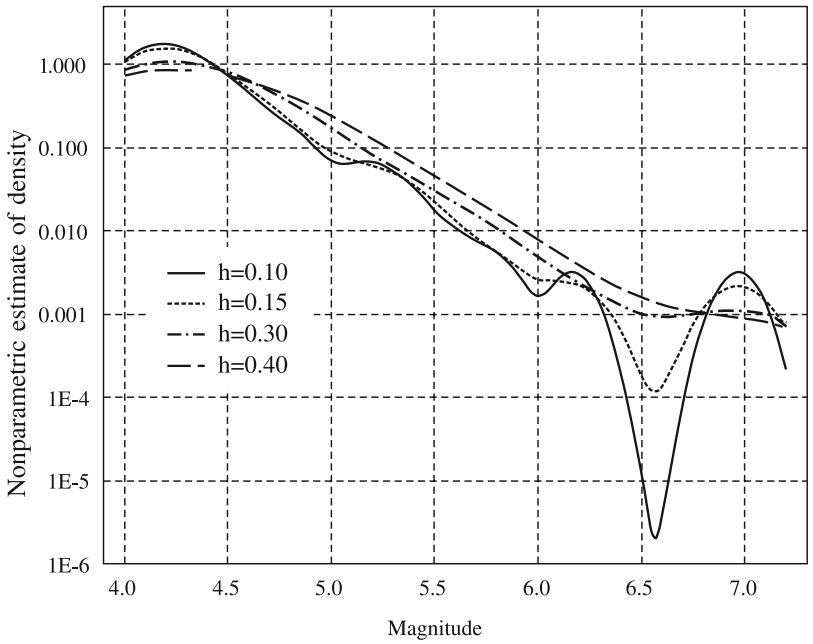

Figure 2. Nonparametric kernel estimate of magnitude density for four different values of the smoothing factor. When h increases, local maxima and inflexion points disappear.

importance of modes and bumps relies on the fact that the multiple occurrences of these features in a probability density indicate, for most standard densities, a mixing of components [*Cox*, 1966]. *Silverman* [1986, and references therein] has developed a nonparametric statistical procedure for testing the number of modes and bumps in a density, called a smooth bootstrap test for multimodality. Using this procedure, we have investigated the complexity of magnitude distribution through a separate testing of the following null hypotheses: H_o^1 (the probability density of magnitude is unimodal) and H_o^2 (the probability density of magnitude has one bump to the right of the mode). The complexity of the tested distribution is evidenced when the significance of either of the null hypotheses is low.

2.2. Testing Procedure

[6] The smoothed bootstrap test for multimodality [*Silverman*, 1986; *Efron and Tibshirani*, 1993] begins from the nonparametric representation of the probability density function of magnitude. Given the sample data $\{M_i\}$, $i = 1,\ldots,n$, the nonparametric kernel estimator of density is

$$\hat{f}(M|\{M_i\},h) = \frac{1}{nh}\sum_{i=1}^{n} K\left(\frac{M-M_i}{h}\right) \tag{1}$$

where h is a positive smoothing factor [e.g., *Silverman*, 1986] and $K()$ is a kernel function. The final shape of the density estimate (equation (1)), in particular the number of modes of $\hat{f}(M|\{M_i\}, h)$ and the number of bumps, strongly depends upon the value of h. For the normal kernel function of the form

$$K(\xi) = \frac{1}{\sqrt{2\pi}}\exp\left(-\xi^2/2\right) \tag{2}$$

which is recommended for this test, the number of modes and the number of bumps are decreasing functions of h (Figure 2). Thus, for any data sample the smallest values of the smoothing factor exist, $h_{cr}(1)$ and $h_{cr}(2)$, such that $\hat{f}(M|\{M_i\}, h)$ has one mode for $h \geq h_{cr}(1)$ and more than one mode for $h < h_{cr}(1)$, and one bump for $h \geq h_{cr}(2)$ and more than one bump for $h < h_{cr}(2)$. The $h_{cr}(l)$, $l = 1, 2$, are called the critical smoothing factors and $\hat{f}(M|\{M_i\}, h_{cr}(l))$, $l = 1, 2$, are used as the estimated null distributions for the tests of our null hypotheses, H_0^1 and H_0^2, respectively. In order to perform the test of either hypothesis R samples of size n, $\{M_i^{(k)}(l)\}$, $i = 1,.,n$, $k = 1,.,R$, are drawn from $\hat{f}(M|\{M_i\}, h_{cr}(l))$ ($l = 1$ or 2). The significance of each of the null hypotheses is estimated as the proportion of its respective samples $\{M_i^{(k)}(l)\}$ that lead to a critical smoothing factor value greater than $h_{cr}(l)$ ($l = 1$ or 2). Alternatively, the significance can be estimated as:

$$P(1) = \left[\text{the number of unimodal } \hat{f}\left(M|\left\{M_i^{(k)}(1)\right\}, h_{cr}(1)\right), \quad k = 1,\ldots,R\right]/R \tag{3a}$$

and

$$P(2) = \left[\text{the number of one bump } \hat{f}\left(M|\left\{M_i^{(k)}(2)\right\}, h_{cr}(2)\right), \quad k = 1,\ldots,R\right]/R \tag{3b}$$

[7] In order to establish the critical smoothing factors we make use of the differentiability of the density estimate (1) with the normal kernel (2) and examine the numbers of zeros of its first and second derivatives, which correspond to the numbers of modes and inflexion points, respectively. Searching $h_{cr}(1)$ for the test for multimodality begins with a small value of h and then h is gradually increased until the

number of zeros of $d\hat{f}(M|\{M_i\}, h)/dM$ become one. We usually apply the step of change of h equal to 0.001, which means that the accuracy of evaluation of the critical smoothing factor is 10^{-3}. For the value of $h_{cr}(1)$ we accept the one before last value of h. The same procedure applied to the second derivative of $\hat{f}(M|\{M_i\}, h)$ provides the $h_{cr}(2)$ value for the test of H_0^2.

[8] Sampling from $\hat{f}(M|\{M_i\}, h_{cr}(l))$ (l = 1 or 2), needed for the evaluation of null hypotheses significances (equations (3a) and (3b)), is done with the smoothed bootstrap technique. For each k, k = 1,.,R, the desired sample $\{M_i^{(k)}(l)\}$, i = 1,.,n (l = 1 or 2) consists of:

$$M_i^{(k)}(l) = M_i' + h_{cr}(l)\varepsilon_i \tag{4}$$

where $\{M_i'\}$ comes from n times uniform selection with replacement from the original data $\{M_i\}$ (standard bootstrap), and ε_i are random numbers from the kernel $K()$, that is, in our case (2), the standard normal random numbers. Finally, the number of zeros of $d\hat{f}(M|\{M_i^{(k)}(1)\}, h_{cr}(1))/dM$ indicates whether the bootstrap sample $\{M_i^{(k)}(1)\}$ leads to unimodal or multimodal $\hat{f}(M|\{M_i^{(k)}(1)\}, h_{cr}(1))$ and the number of zeros of $d^2\hat{f}(M|M_i^{(k)}(2)\}, h_{cr}(2))/dM^2$ indicates whether the bootstrap sample $\{M_i^{(k)}(2)\}$ leads to one bump or multibump $\hat{f}(\mathrm{M}|\{M_i^{(k)}(2)\}, h_{cr}(2))$.

[9] The larger the sample variance, the larger the critical smoothing factor. *Silverman* [1986] and *Efron and Tibshirani* [1993] point to the fact that sampling according to equation (4) increases artificially the variance of the bootstrap samples $\{M_i^{(k)}(l)\}$ compared to the variance of the original data sample $\{M_i\}$. This leads to an artificial increase in the significance of the null hypotheses (equations (3a) and (3b)). To avoid this effect, *Efron and Tibshirani* [1993] recommend the replacement of $\{M_i^{(k)}(l)\}$ in this test by

$$M_i^{(k)^*}(l) = \overline{M}^{(k)}(l) + \left(M_i^{(k)}(l) - \overline{M}^{(k)}(l)\right) \Big/ \left(1 + h_{cr}(l)^2/\hat{\sigma}^2\right)^{0.5} \qquad i = 1, \ldots, n \tag{5}$$

where $\overline{M}^{(k)}(l)$ is the mean of $M_1^{(k)}(l),\ldots,M_n^{(k)}(l)$, and $\hat{\sigma}^2$ is the sample variance of $\{M_i\}$. The $\{M_i^{(k)^*}(l)\}$ have approximately the same variance as the data sample $\{M_i\}$.

2.3. Test Calibration

[10] The works on the smooth-bootstrap test for multimodality cited in the previous section consider normal or normal-like distributions. Earthquake magnitudes are controlled by exponential-like distributions. Therefore, before applying the smooth-bootstrap test to real magnitude data, we made a series of Monte Carlo experiments determining its effectiveness in investigating properties of the exponential distributions. The experiments were based upon the notion of the null hypothesis significance, which is the probability of type I error: to reject H_o when it is true. Suppose a null hypothesis, H_o, is true in a population. Let H_o be tested on N samples drawn from this population, and let N be large. If the applied test works correctly, then for any $p \in (0,1)$ the number of samples, ν, upon which the estimated H_o significance is $\leq p$ should be about $N \times p$. If $\nu < N \times p$ then the test, when applied to a real data sample, overestimates the significance of the null hypothesis. An underestimation occurs for the reversed relation.

[11] In the considered problem the Monte Carlo technique was used to draw samples from the both-side truncated exponential distribution, which is one of the most popular models for magnitude [*Page*, 1968; *Cosentino et al.*, 1977]. Its cumulative distribution function (CDF) is

$$F(M|M_{\max}) = \begin{cases} 0, & M < M_c \\ \dfrac{1 - \exp[-\beta(M - M_c)]}{1 - \exp[-\beta(M_{\max} - M_c)]} & M_c \leq M \leq M_{\max} \\ 1, & M > M_{\max} \end{cases} \tag{6}$$

where β, M_c, $M_{\max}$, are distribution parameters. M_c represents the threshold of catalog completeness, $M_{\max}$ is the upper limit of magnitude range and $\beta = b\log 10$, where b is the Gutenberg-Richter b value. It was then found out that the test for H_o^1 (modality) without correction of variance (equation (5)), when applied to the generated samples, usually overestimated the significance of the null hypothesis. This effect appeared most often in the most interesting from our standpoint range of small significance of the null hypothesis. When the variance correction (equation (5)) was applied, the test for H_o^1 provided usually correct estimates of H_o^1 significance. Occasionally, however, a tendency for diminishing the significance of the null hypothesis H_o^1 was also observed. When testing for the number of bumps (H_o^2) without correction (equation (5)), a slight underestimation of the null hypothesis significance could occur. The test for H_o^2 with correction (equation (5)) strongly underestimated the significance of H_o^2. In the light of these results, it was decided that correction (equation (5)) would be applied in testing for H_o^1 but not in testing for H_o^2. Moreover, in order to avoid drawing false conclusions, computer simulations were used to calibrate every result indicating the low significance of either of the null hypotheses. Calibrating means rescaling the H_o significance, determined by the test, to the significance, which is actually hidden in the data sample. Let H_o (H_o^1 or H_o^2) significance, estimated by the smoothed bootstrap test from an actual data sample $\{M\}$, be p^*. In order to rescale p^* we must have N standard samples drawn from a distribution, which (1) supports the H_0 hypothesis and (2) could underlay the actual data. The rescaled estimate of significance is the proportion of the standard samples for which the significance estimated by the test is less than or equal to p^*.

[12] The standard samples were drawn from the exponential distribution (equation (6)) by means of the Monte Carlo technique. To ensure desired similarity between the data sample and the standard samples, M_c was set to the actual completeness level of the studied earthquake data and β and $M_{\max}$ were estimated from the data sample, $\{M\}$. The β was estimated with the maximum likelihood method and for $M_{\max}$ assessment we used a generic formula of *Kijko and Graham* [1998]:

$$\hat{M}_{\max} = M_{\max}^{obs} + \int_{M_c}^{\hat{M}_{\max}} [F(M|M_{\max})]^n \mathrm{d}M \tag{7}$$

where $M_{\max}^{obs} = \max(\{M\})$ and n is the size of $\{M\}$. In every case 1000 standard samples were generated. An example of the test calibration results is shown in Figure 3. The estimated significance, p^*, of the H_o^1 hypothesis for one of the actual samples is plotted against the empirical cumulative distribution function of the significance estimate that is the proportion of samples for which the significance estimated by the test is less than or equal to p^*. For an ideal test, the result should be the bisector ($y = x$). This can be observed from Figure 3; the test in this presented case was conservative for $p^* < 0.8$.

2.4. Approximate Location of the Break in Magnitude Scaling

[13] When the complexity of the magnitude distribution is supposed to take the form of a bi−log linear frequency-magnitude relation, the location of the kink on the magnitude scale is interpreted in connection with the parameters of the seismogenic zone [e.g., *Triep and Sykes*, 1997; *Aki*, 2000; *Knopoff*, 2000; *Stock and Smith*, 2000; *Klein et al.*, 2001]. This break in magnitude scaling in an area is expected to occur at a point where the dimension of the event equals the downdip width of the seismogenic layer [*Pacheco et al.*, 1992]. Such breaking is different in various seismotectonic environments, depending upon how many faults exist and how large they are. For the whole territory of Greece, this breaking is at $M7.0$, meaning that faults capable generating events with $M \geq 7.0$, are rare in comparison with those connected with smaller events [*Papazachos and Papazachou*, 2003]. For individual smaller seismogenic zones, which constitute systems containing many faults, like the ones studied here that are subsets of the Greek territory, this point is expected to vary though constituting smaller magnitude values. The fact that the larger and smaller earthquakes have different size distributions has important implications for earthquake hazard analysis, which often relies on predicting the former from the extrapolation of the later.

[14] In our approach, neither the bilog linear nor any other specific model of complexity is assumed. Nevertheless, after ascertaining that the magnitude distribution is complex, information on the locations of nonlinear features in the distribution can lead to a better understanding of the earthquake process.

[15] As mentioned in section 2.2, the number of modes and the number of bumps in the kernel estimate of magnitude density (equation (1)) are decreasing functions of the smoothing factor, h. As long as h is greater than its critical value for the number of modes, $h_{cr}(1)$, the density estimate has a unimodal form. When h becomes a little less than $h_{cr}(1)$ the density estimate becomes bimodal and the first derivative of the density estimate has three zeros: the first assigns the primary mode, the second the minimum between the modes, and the third one the secondary mode. If the test for multimodality indicates bimodality of the magnitude distribution, these features of the estimate are most likely related to the features of this distribution. In this work, the second zero of the first derivative of the density estimate, that is the local minimum of the density estimate, is considered as the location of a break in magnitude scaling. Unfortunately, for different values of h ($h \leq h_{cr}(1)$) the minimum of the density estimate locates itself at slightly different points. These variations of location of the minimum are usually insignificant, one to two tenths in magnitude units (MU), but occasionally we observe a "floating" of the local minimum over a larger range, up to 0.5 MU. Thus the procedure provides only an approximate position of the minimum separating the primary and secondary modes.

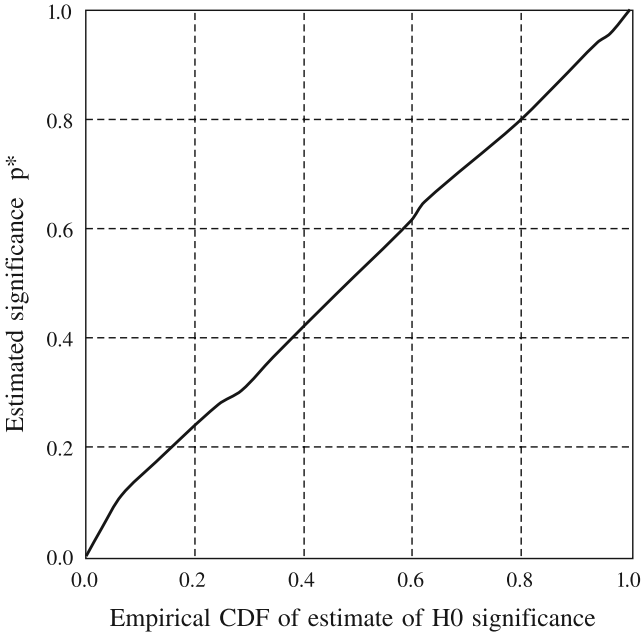

Figure 3. An example of calibration of the smooth bootstrap test for multimodality. The empirical cumulative distribution function of the estimate of H_0 significance is the proportion of the standard samples, for which the estimated significance of $H_0 \leq p^*$.

3. Seismotectonic Regime of the Study Area

[16] Various researchers have presented much information on basic problems regarding active tectonics and deformation in the broader Aegean area (Figure 4). It is one of the most active tectonic regions of the Alpine-Himalayan belt, with its most prominent tectonic feature being the subduction of the eastern Mediterranean lithosphere under the Aegean Sea along the Hellenic Arc [*Papazachos and Comninakis*, 1970, 1971]. Seismicity is very high throughout the arc, which is dominated by thrust faulting with a NE-SW direction of the axis of maximum compression. A belt of thrust faulting runs along the eastern Adriatic shore, continues south along the coastal regions of Albania and northwestern Greece and terminates at the central Ionian Islands. Thrust faulting is connected with the continental collision between Outer Hellenides and the Adriatic microplate. The direction of the maximum compression axis is almost normal to the direction of the Adriatico-Ionian geological zone. Between the continental collision to the north and oceanic subduction to the south, the dextral strike-slip Cephalonia Transform Fault (CTF) is observed in the area of the central Ionian Islands [*Scordilis et al.*, 1985]. This is in agreement with the known relative motion of the Aegean and eastern Mediterranean.

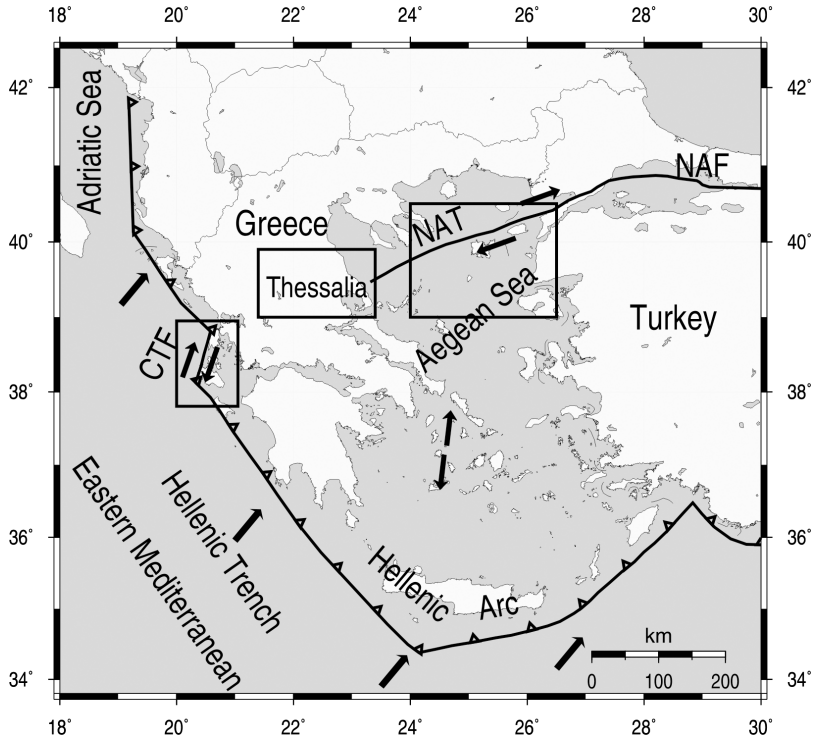

Figure 4. Main seismotectonic properties of the broader Aegean region. NAF, North Anatolia Fault; NAT, North Aegean Trough; CTF, Cephalonia Transform Fault. The rectangles indicate the studied areas.

[17] The back-arc area, south Aegean Sea and continental Greece is dominated by extension. The north Aegean Sea is characterized by a combination of a right-lateral shear and extension. *McKenzie* [1970, 1972, 1978] showed that the northward motion of the Arabian plate pushes the smaller Anatolian plate westward along the North Anatolian fault, continuing along the North Aegean Trough (NAT) region, which is the boundary between the Eurasian and south Aegean plates. The right-lateral strike-slip motion associated with the North Anatolian Fault (NAF) appears to become more distributed in the northern Aegean Sea. This motion is transferred into the Aegean but in a southwesterly direction. This style of faulting is consistent with several fault plane solutions of recent strong earthquakes [*Papazachos et al.*, 1998].

[18] Three areas, which are amongst the most active ones in the territory of Greece were selected for the current analysis (Figure 4), namely, the central Ionian Islands, Thessalia and the northern Aegean Sea. The central Ionian Islands area has both a high level of seismic activity along an active boundary and a record of earthquakes complete from M_c6.0, extending back to at least 1850. Historical data show that the seismicity rate of strong ($M \geq 6.5$) main shocks in this zone has remained stable during the last four centuries with an average of about one such shock per decade [*Papadimitriou and Papazachos*, 1985]. Several large ($M \geq 7$) events have repeatedly destroyed urban areas as has been reported historically, while the smaller magnitude earthquakes ($6 \leq M \leq 7$) that have occurred during the instrumental era, that is since the beginning of the 20th century, have also produced extensive damage and loss of life. Four active periods have been observed since 1867 after analyzing the spatial-temporal distribution of shallow strong ($M \geq 6.3$) earthquakes, alternating with much longer relatively quiescent periods. Each active period consists of a relatively large event or series (two to four) of events occurring closely in space and time, and has been interpreted on the basis of triggering between adjacent fault segments [*Papadimitriou*, 2002].

[19] The Thessalia area belongs to the extensional back-arc Aegean region and is characterized by extension on subparallel normal faults. From 1954 until 1958, five strong ($6.2 \leq M \leq 7.0$) earthquakes devastated towns and villages located along the southwestern border of the Thessalia basin. This remarkable sequence took place on along-strike normal faults interacting through their stress fields [*Papadimitriou and Karakostas*, 2003].

[20] The Northern Aegean Trough (NAT in Figure 4) constitutes the northern boundary of the south Aegean plate [*Papazachos et al.*, 1998] and is a continuation of the western part of the North Anatolian fault. Dextral strike-slip faulting dominates the northern Aegean Sea area as the North Anatolian fault prolongates into the northern Aegean Sea, where it bifurcates into two main branches of the NE-SW trend. Parallel secondary faults are also recognized from seismicity and fault plane solutions of recent strong earthquakes. This area has frequently experienced many destructive earthquakes ($M \geq 7.0$), some of them occurring very close in time, as indicated from both instrumental data and historical information. The spatial and temporal occurrence patterns of these events were examined by stress changes associated with the occurrence of each of them, and it was revealed that the triggering of subsequent ones

Table 1. Information on the Data Samples Used in the Analysis

Sample	Origin: Area	Origin: Time Period	Sample Size	Magnitude Range
CI50	Central Ionian Islands	1911–2001	167	[5.0, 7.2]
CI45	Central Ionian Islands	1950–2001	563	[4.5, 7.2]
CI43	Central Ionian Islands	1964–2001	867	[4.3, 7.0]
CI40	Central Ionian Islands	1981–2001	1256	[4.0, 7.0]
TH50	Thessalia	1911–2001	62	[5.0, 7.0]
TH45	Thessalia	1950–2001	190	[4.5, 7.0]
TH43	Thessalia	1964–2001	177	[4.3, 6.5]
TH40	Thessalia	1981–2001	104	[4.0, 5.6]
NA50	Northern Aegean Sea	1911–2001	82	[5.0, 7.2]
NA45	Northern Aegean Sea	1950–2001	311	[4.5, 7.2]
NA43	Northern Aegean Sea	1964–2001	514	[4.3, 7.2]
NA40	Northern Aegean Sea	1981–2001	744	[4.0, 7.2]

explains the occurrences of large earthquakes [*Nalbant et al.*, 1998; *Papadimitriou and Sykes*, 2001].

4. Data

[21] The data for the present study were obtained from the catalog of the earthquakes that have occurred since the beginning of the 20th century in the broader Aegean region [*Papazachos et al.*, 2005]. The catalog is homogeneous, as all magnitudes are expressed as equivalent moment magnitudes [*Papazachos et al.*, 1997] and is complete from M_c5.0 since 1911, M_c4.5 since 1950, M_c4.3 since 1964, and M_c4.0 since 1981. The catalog data from each of the areas under study, namely, the central Ionian Islands, Thessalia and the northern Aegean Sea, were used to construct four samples linked to these completeness levels, respectively. In every case, the first sample comprised magnitudes of events from the longest time period (1911–2001) and the narrowest magnitude range ($M \geq 5.0$), and the fourth sample comprised magnitudes of events from the shortest time period (1981–2001) and the widest magnitude range ($M \geq 4.0$). The selected data samples are presented in Table 1.

[22] The kernel density estimator (equation (1)) has been introduced for continuous random variables that preclude the occurrence of repeated values in a sample. Since earthquake magnitudes are given with one digit after the decimal point, many values in the selected samples were the same. The repeated values would produce spurious local irregularities (modes and bumps) on the kernel density estimate. Therefore, to ensure the proper performance of the kernel estimation, magnitudes were randomized within their round-off interval of length 0.1. In practice, the magnitude estimation error is greater than one tenth and can be about 0.3. Thus it might be more reasonable to randomize magnitudes in an interval of a length 0.3. In this work, however, we did not want to change the data more than the minimum required for the applicability of the nonparametric estimation. The data randomized within 0.1 when rounded off to one tenth became identical with the original data. This would not be the case if a longer interval of randomization were used and could raise discussion on how much such randomization has changed the observed magnitude-frequency distribution. Therefore an analysis of influence of data accuracy on the magnitude distribution complexity study results is left for a subsequent work.

[23] The randomization is obtained through the following transformation of the measured value M:

$$M_{sh} = F^{-1}\{u[F(M + 0.5\delta M) - F(M - 0.5\delta M)] + F(M - 0.5\delta M)\} \quad (8)$$

where δM is the length of the interval of randomization, in our case equal to 0.1, u is a random value from the uniform distribution (0,1), $F()$ is the cumulative function of the distribution of actual values within the round-off interval and $F^{-1}()$ is its antifunction. In the present work, we have assumed that the magnitude distribution within the round-off intervals was exponential of the cumulative distribution:

$$F(M) = 1 - \exp[-\beta(M - M_c)] \quad (9)$$

where β was the maximum likelihood estimate for the whole data sample and M_c was the lower bound of the sample data. There were two reasons behind this choice of the model of randomization. First, the exponential distribution is an option for the probabilistic origin of the sample data, for which the tested null hypotheses are true. Therefore such a model of randomization has always increased the significance of the null hypotheses; thence did not help to conclude on the complexity of the magnitude distribution. Second, thanks to the way β was selected, the data within every round-off interval were statistically similar to the whole sample and the randomization did not produce any artificial irregularities (additional modes or bumps) in the magnitude density.

5. Test Results

[24] The significances of the considered null hypotheses were estimated using, in every case, 1000 smoothed bootstrap samples (equation (3a) and (3b)). When the estimated significance of either hypothesis was less than 0.1, which could suggest that the hypothesis was not true, the test results, presented in Table 2, were calibrated using 1000 standard samples as described in section 2.3.

[25] The locations of the breaks in magnitude scaling were evaluated only for data where the calibrated significance of either of the null hypotheses was low, that is for the earthquake data from the central Ionian Islands and from the

Table 2. Results of Verification of the Null Hypotheses on Magnitude Distribution[a]

Sample	Sample Size	Significance of H_o[1b]	Significance of H_o[2c]
CI50	167	0.19	0.31
CI45	563	0.18	0.29
CI43	867	**0.15**	**0.31**
CI40	1256	**0.069**	**0.08**
TH50	62	0.82	0.81
TH45	190	0.81	0.43
TH43	177	**0.56**	**0.30**
TH40	104	**0.51**	**0.23**
NA50	82	**<0.048**	**<0.06**
NA45	311	**0.056**	**<0.064**
NA43	514	**0.047**	**0.062**
NA40	744	**0.049**	**0.076**

[a]Values in bold are calibrated.
[b]The magnitude density is unimodal.
[c]The magnitude density has one bump.

northern Aegean Sea. The approximate location of the break for the central Ionian Islands data was at M6.5–6.6. The location of the break for the northern Aegean Sea data was at M6.15–6.20.

6. Discussion

[26] The result of the smoothed bootstrap test for multimodality is p, the significance of the tested null hypothesis, either H_o^1 or H_o^2, that is the probability of making an error when rejecting the null hypothesis. The test does not provide any estimate of the probability of making an error when accepting the null hypothesis. Thus its result is conclusive only when p is low, suggesting that one should reject the null hypothesis and accept its alternative, while a higher p does not signify the correctness of H_o. Moreover, the p estimate is linked to the tested sample, hence its high value stems either from the fact that the null hypothesis is true or is caused by the sample deficiencies such as too narrow an interval of variability or too small a size. If the latter is true then testing a more representative sample of the same population should result in reducing p.

[27] In connection with the above remarks, the most conclusive results have been obtained for data from the northern Aegean Sea area (NA samples, Table 2). The magnitude distribution complexity has been indicated (with 5–8% probability of error) by both tests performed on every data sample from this region. The magnitude density is very likely bimodal at least.

[28] For only one sample of the data from the central Ionian Islands area (CI samples, Table 2), namely, the CI40, was the calibrated significance of the null hypotheses fairly low. Nevertheless, in the light of the above remarks on the dependence of the estimated null hypothesis significance on sample properties, the result for CI40 signifies the complexity of the magnitude distribution in the central Ionian Islands regardless of the results for the other three CI samples. Remarkably, the sample that supported the complexity hypothesis was from the most recent part of the catalog with a magnitude cutoff equal to 4.0. This sample better reflected the complexity of the underlying distribution than the other ones probably because it covered a wider magnitude range. The other possible explanation of the test results for the central Ionian Islands samples is that these samples were not drawn from the same distribution. It would mean that the magnitude distribution for this area was significantly time varied for the period 1911–2001.

[29] The test results for the data from the Thessalia area (TH samples, Table 2) do not constitute grounds to reject either of the null hypotheses, and conclude that the magnitude distribution underlying the data is not smoothly non–log linear but is more complex. This may be due to either the actual simplicity of the distribution or the small sizes and more narrow magnitude ranges of the samples in comparison with the previous two cases (Table 1). The largest sample from this area comprised only 190 events, and the magnitude range varied from 1.6 to 2.5, whereas for the central Ionian Islands and northern Aegean Sea this range was between 2.2–3.0 and 2.3–3.2, respectively.

[30] From a seismotectonic point of view, the rapidly deformed northern Aegean Sea area embodies more than one distinctive parallel dextral strike-slip fault zone, which failed several times during the period that our study covers. This resulted in the inclusion of an adequate number of $M >$ 6.2 events. The "deficit" in the events at about $M = 6.2$ (the local minimum of the estimated magnitude density) compared with the larger magnitudes may be plausibly attributed to fault growth by the coalescence of smaller fault segments, since increasing deformation within the fault zone leads to an overall smoothing of fault zone topography [*Scholz*, 2002]. Thus the number of distinct smaller fault segments decreases after repeated slipping. Magnitude complexity is not so pronounced for the central Ionian Islands area, although coalescence could also prevail since this area exhibits the highest strain rate in the whole territory of Greece [*Papazachos and Kiratzi*, 1996]. The fact that features of complexity in the magnitude distribution are not as distinct for this area as they are for the northern Aegean Sea area may be due to the more frequent occurrence of events in all magnitude ranges (two to three times the number for the northern Aegean Sea and Thessalia areas, respectively) that probably smoothes the distribution. This area comprises a dextral strike-slip fault zone bounded by continental collision on its northern boundary and oceanic subduction on its southern boundary, as is mentioned above. Temporal variation of the magnitude distribution may be associated with the time clustering of seismic excitations along this individual fault zone. The area of Thessalia is seismically less active than the other two areas examined, with only one event of M7.0, which is the maximum magnitude ever reported even in historical records, but with 12 events in the magnitude range $6.0 \leq M \leq 6.9$ for the years 1911–2002. This suggests that fault segmentation dominates the mode of active deformation, resulting in a simpler distribution in the rightward portion of the magnitude range.

7. Implications for Probabilistic Seismic Hazard Assessment

[31] The probabilistic properties of a seismic source zone are often characterized by the probability of the occurrence of an event with magnitude M_p or more in a period of D time units. If the earthquake process is Poissonian this probability is given by:

$$R(M_P, D) = 1 - \exp\{-\lambda D[1 - F(M_P)]\} \tag{10}$$

where λ is the mean event rate and $F()$ is the cumulative distribution function (CDF) of magnitude. The mean return period of events of magnitude M_P is

$$T(M_P) = \{\lambda[1 - F(M_P)]\}^{-1} \tag{11}$$

It is obvious that an accurate estimation of the magnitude CDF, $F(M)$, is crucial for a proper assessment of these parameters. Magnitude distribution models commonly used in seismic hazard analysis are at most smoothly non–log linear, and when applied to represent a complex magnitude distribution can generate large systematic errors of hazard parameters. *Lasocki et al.* [2000, 2002] and *Kijko et al.* [2001] proposed to overcome the problem of the improper modeling of magnitude distribution by applying a model-

free approach to the probabilistic characterization of a seismic source for seismic hazard analysis, based on the kernel nonparametric estimators of the unknown probability functions of magnitude. The presently used nonparametric estimator of magnitude CDF has the form:

$$\hat{F}^*(M) = \frac{\sum_{i=1}^{n}\left[\Phi\left(\frac{M-M_i}{\alpha_i h}\right) - \Phi\left(\frac{M_c-M_i}{\alpha_i h}\right)\right]}{\sum_{i=1}^{n}\left[\Phi\left(\frac{M_{\max}-M_i}{\alpha_i h}\right) - \Phi\left(\frac{M_c-M_i}{\alpha_i h}\right)\right]}, \qquad (12)$$

$$M_c \le M \le M_{\max}$$

where M_c is the threshold of catalog completeness, M_i, i = 1,..,n are observed magnitudes such that $M_i \ge M_c$, n is the size of the complete part of the catalog, $M_{\max}$ is the upper limit of the magnitude range, $\Phi()$ is the CDF of standard Gaussian distribution, h is the smoothing factor and α_i, i = 1,..,n are the local bandwidth factors. The $M_{\max}$ is estimated according to (7). As presented in section 2.2 the shape of the kernel estimates depends primarily on the value of the smoothing factor h. From the point of view of the use of a CDF estimator (equation (12)) in the hazard analysis, a global, integrant agreement between the actual density and its estimates is of the utmost importance. Therefore h is selected by means of the least squares cross-validation technique that requires minimizing the integral of the squared difference between the actual density, $f(\xi)$, and the estimate, $\hat{f}(\xi)$: $\int_{-\infty}^{\infty}\left[\hat{f}(\xi) - f(\xi)\right]^2 d\xi$ [e.g., *Bowman et al.*, 1984]. *Kijko et al.* [2001] showed that in the case of the Gaussian kernel this criterion is fulfilled if h is the root of the equation

$$\sum_{i,j}\left\{2^{-0.5}\left[\frac{(M_i-M_j)^2}{2h^2}-1\right]\exp\left[-\frac{(M_i-M_j)^2}{4h^2}\right] - 2\left[\frac{(M_i-M_j)^2}{h^2}-1\right]\exp\left[-\frac{(M_i-M_j)^2}{2h^2}\right]\right\} - 2n = 0 \qquad (13)$$

The local bandwidth factors, $\{\alpha_i\}$ widen the kernels associated with data points from the range where the data are sparse [*Orlecka-Sikora and Lasocki*, 2005]. The factors are

$$\alpha_i = \left[\frac{\hat{f}(M_i|\{M_i\},h)}{g}\right]^{-0.5} \qquad (14)$$

where $\hat{f}(\bullet|\{M_i\}, h)$ is the pilot, constant kernel estimator in the unbounded magnitude range (equations (1) and (13)) and

$$g = \left[\prod_{i=1}^{n}\hat{f}(M_i|\{M_i\},h)\right]^{\frac{1}{n}}$$

is the geometric mean of all constant kernel estimates (For a detailed description of the bandwidth factors and a justification of their use, see *Silverman* [1986].) Studies of the efficiency of this approach to seismic hazard estimation, performed on simulated data, showed that it provides results with tolerable, limited errors regardless of whether the actual magnitude distribution follows the Gutenberg-Richter relation or is complex [*Kijko et al.*, 2001]. Therefore it is particularly suitable for analyzing sample data that signify, through the smoothed bootstrap test for multimodality, complexity of the underlying magnitude distribution. It was also shown in the cited work of *Kijko et al.* [2001] that to the contrary, the classic magnitude CDF estimators that use smooth parametric models for magnitude (e.g., equation (6)) fail when the distribution is complex. Thus the significant differences between the classic and nonparametric estimates of the seismic hazard parameters indicate the complexity of the magnitude distribution.

[32] In order to demonstrate the implications of magnitude distribution complexity on seismic hazard evaluation, we estimated the magnitude CDFs (equation (12)) and the mean return periods (equation (11)) applying the classic and nonparametric approach to data samples from the study areas. The processed samples from the central Ionian Island and northern Aegean Sea areas were CI40 and NA40, respectively, that is those from the last 20-year part of the catalog, which had the lowest cutoff value, equal to 4.0. Because the nonparametric estimates of hazard parameters become considerably uncertain when the sample size is less than about 130 elements and the sample from the years 1981–2001 from Thessalia area comprised only 104 elements we analyzed in this case the sample covering a longer period, i.e., 1964–2001 with a cutoff magnitude equal to 4.3 (TH43). In all cases, the doubly truncated exponential distribution (equation (6)) was used as a model for magnitude in the classic approach.

[33] The estimates of magnitude CDFs and the respective cumulative histograms of observed magnitudes are shown in Figure 5. Regarding the whole magnitude range, the differences between nonparametric and parametric estimates do not seem to be significant, becoming invisible in the case of the northern Aegean Sea data. Both estimates fit the observed data well. A magnified view of the larger magnitude range shows, however, some differences between these estimates. In general, the nonparametric estimate follows subtle changes of the histogram whereas these changes are ignored by the parametric estimate.

[34] The formula for the mean return period contains the expression $1 - F(M_p)$ in the denominator (equation (11)). When M_p is large, that is the mean return period of strong earthquakes is considered, this expression is close to zero and even slight inaccuracy of its estimate has a very strong effect on the return period estimation error. The influence of the small differences between the nonparametric and parametric CDF estimates on the return period estimates is presented in Figure 6. The parametric and nonparametric estimates for the central Ionian Islands area (Figure 6a) are similar below magnitude 4.5. In the magnitude range [4.5, 6.3] the nonparametric estimate of the return period is slightly larger than its parametric counterpart. To the contrary, in the magnitude range [6.3, 7.2] the linear model for magnitude causes a significant overestimation of the return period compared to the nonparametric result. This subsequently results in underestimation of the exceedance probability (equation (10)). Above magnitude 7.2 both estimates quickly approach their asymptotic limits.

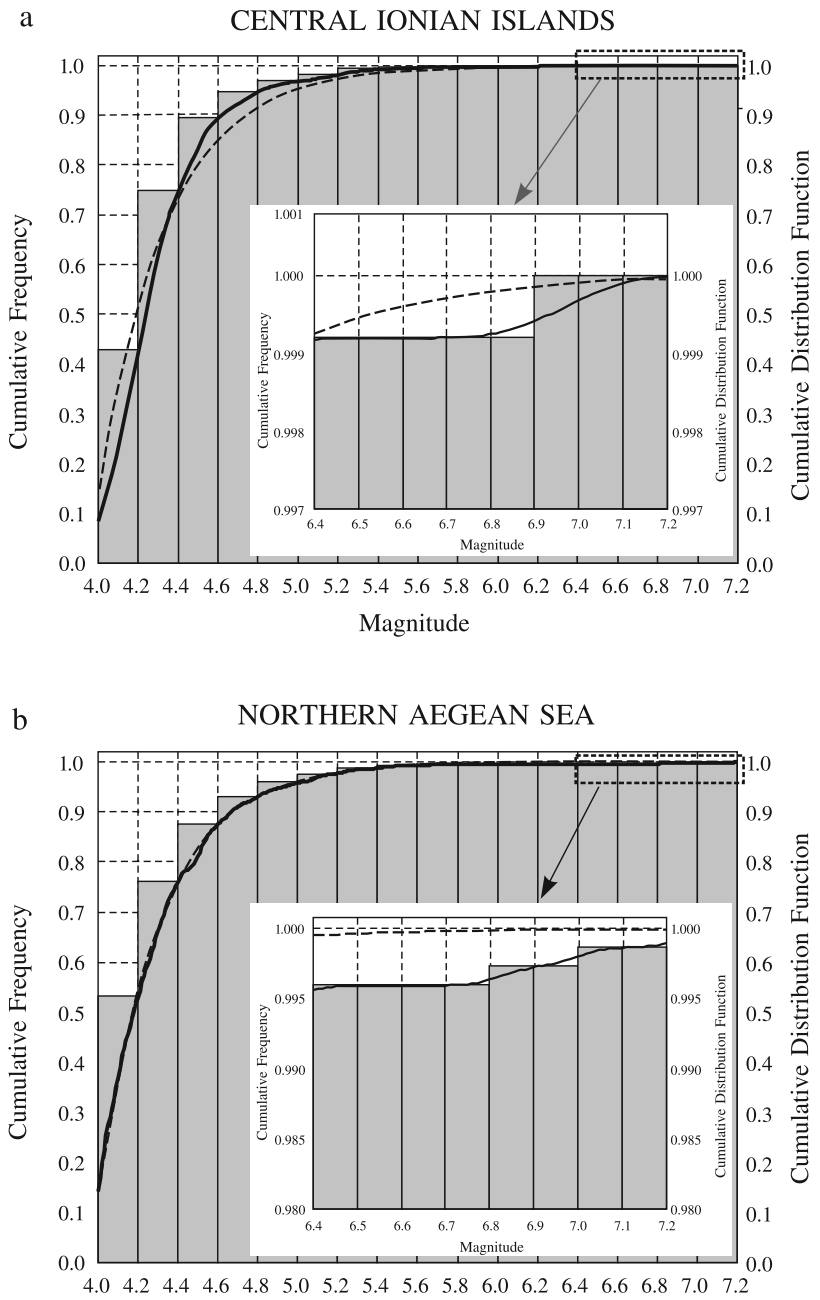

Figure 5. (a) A cumulative histogram of observed magnitudes and estimates of the magnitude cumulative distribution function for the central Ionian Islands area. The nonparametric estimates are represented by the continuous line and the classic (parametric) estimates are represented by the dotted line. (b) Same as in Figure 5a for the northern Aegean Sea area. (c) Same as in Figure 5a for the Thessalia area.

[35] The parametric and nonparametric return period estimates for the northern Aegean Sea area (Figure 6b) for smaller magnitudes up to 5.6–5.7, are practically the same. For magnitudes >5.7 the rate of increase of the parametric estimate is much greater than that for the nonparametric estimate, such that the difference between these two estimates becomes very big. For example, for M = 6.7 the nonparametric estimate of the return period is 7 years and the parametric estimate is 145 years. Starting from a magnitude of about 7.3, the nonparametric return period gradually approaches its asymptote while the parametric one continues its linear trend.

[36] Although the complexity of the magnitude distribution for earthquakes from the Thessalia area has not been ascertained by the smoothed bootstrap test, differences between the nonparametric and parametric return period estimates are also significant in this case (Figure 6c). For magnitudes from 5.5 to 6.5, the nonparametric return period is from 1.1 to about 4 times smaller than the parametric estimate.

[37] As already mentioned, the Monte Carlo simulation studies of the nonparametric kernel estimators of magnitude distribution functions [*Kijko et al.*, 2001] have indicated that the differences between the nonparametric and parametric

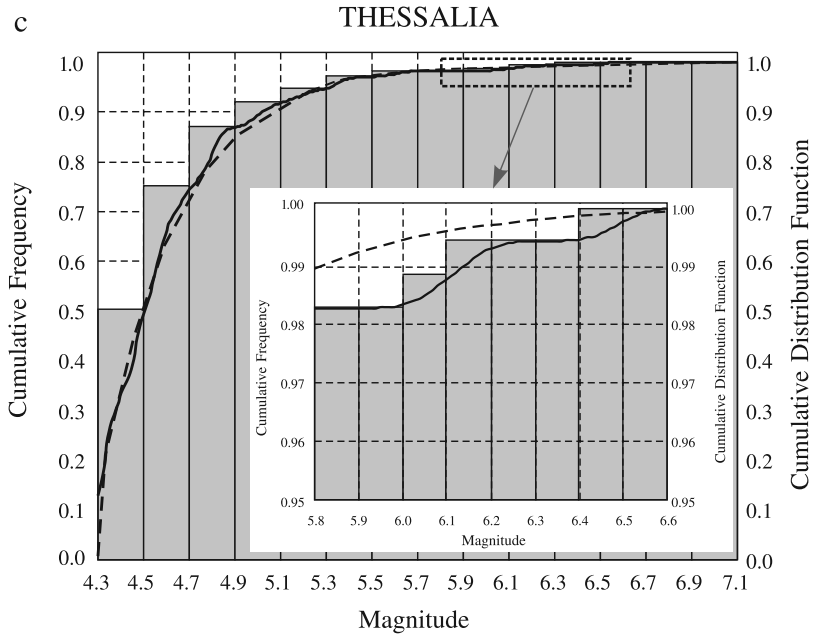

Figure 5. (continued)

CDF estimates and the subsequent differences between the nonparametric and parametric return period estimates occurred only when the distribution that underlay observations was not smoothly non–log linear but was more complex. In such cases, the nonparametric estimates were those ones that fitted correctly the actual CDF and return period, respectively. On the basis of these results we have more confidence, in the present study, in the nonparametric estimates than in the parametric ones. Besides, it was also possible to validate the results presented in Figure 6 directly with the observed earthquake data. The return period estimates in Figure 6 were obtained from the earthquake data for 20 and 38 years periods, namely, from 1981 to 2001 for the central Ionian Island and northern Aegean Sea areas and from 1964 to 2001 for the Thessalia area. We had in hand, however, reliable information on earthquakes of magnitudes greater than or equal to 5.0 from the much longer time interval of 1911–2004 (94 years). These data covered narrow ranges of magnitudes and were few in number and therefore were not used to estimate the magni-

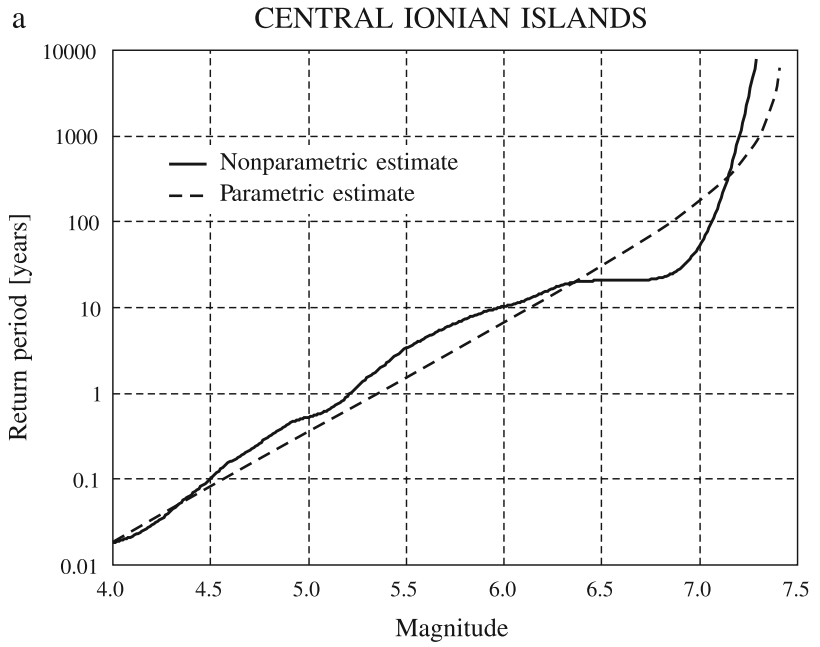

Figure 6. (a) Estimates of the earthquake mean return period for the central Ionian Islands area. The nonparametric estimates are represented by the continuous line and the classic (parametric) estimates are represented by the dotted line. (b) Same as in Figure 6a for the northern Aegean Sea area. (c) Same as in Figure 6a for the Thessalia area.

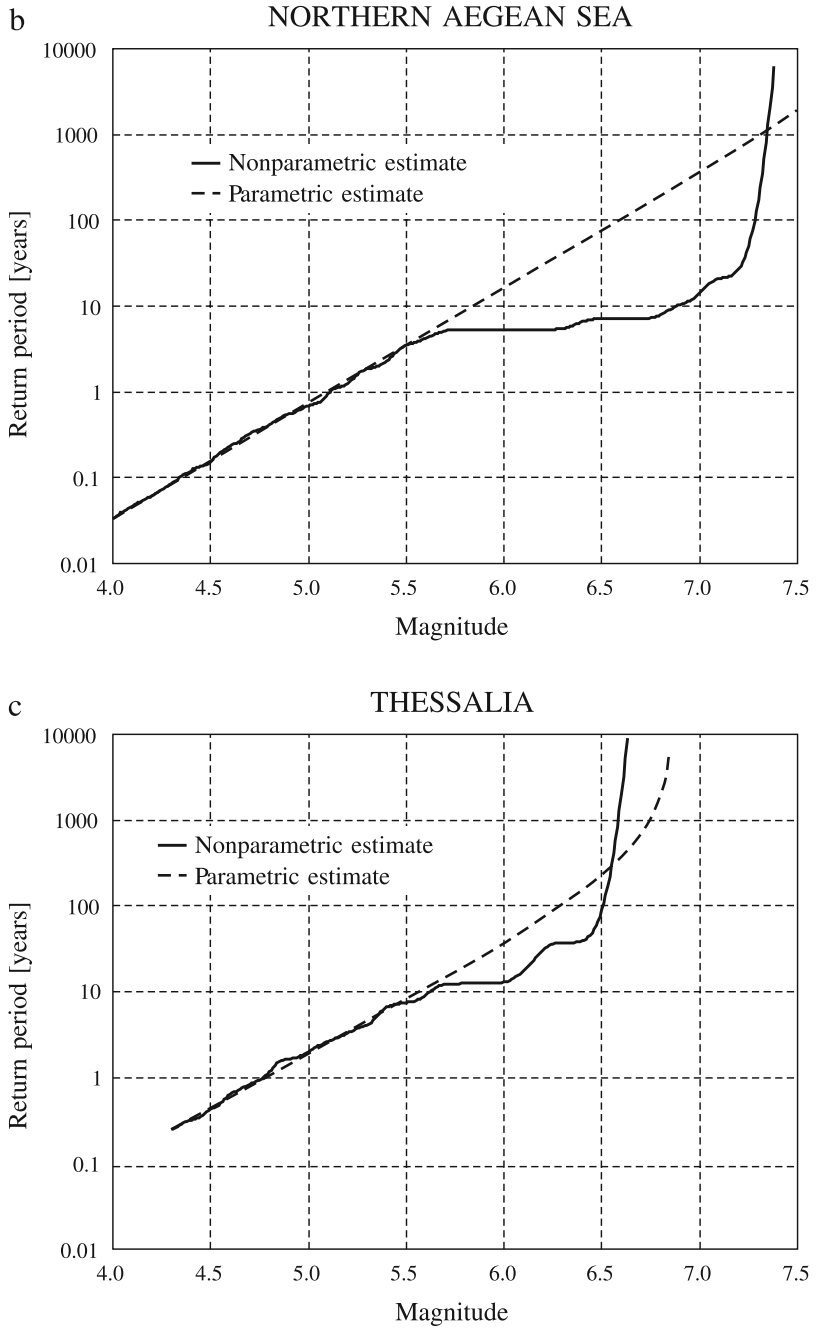

Figure 6. (continued)

tude CDF (equation (12)) and the mean return period (equation (11)) because the nonparametric estimates would be inaccurate. These data could be, however, used to estimate the mean return period of the larger earthquakes by the ratio of 94 years to the number of occurrences of target events. A comparison between this estimate, further termed 'observational', and the parametric and nonparametric results is presented in Figure 7.

[38] There is not much difference between the three return period estimates for magnitudes 5.0, 5.5, and 6.0 for the central Ionian Islands area (Figure 7a). For magnitude 6.5, the parametric estimate deviates more significantly from the observational and nonparametric estimates, which are more or less alike. This difference becomes very large for magnitude 7.0; the parametric return period, being equal to 174 years, is more than 3 times greater than either of the observational and nonparametric estimates, being equal to 53 and 47 years, respectively. The return period estimates for the northern Aegean Sea area (Figure 7b) also do not differ up to magnitude 6.0. For magnitude 6.5, however, the parametric estimate is much greater than the nonparametric and observational ones. For magnitude 7.0, the difference is extreme: the parametric estimate is 371 years while the nonparametric and observational ones are 14 and 31 years, respectively. In summary, one can conclude for these two seismotectonic areas that if the observational return period estimate can be treated as a reference, then the parametric estimate evaluated from the data from 20 years period

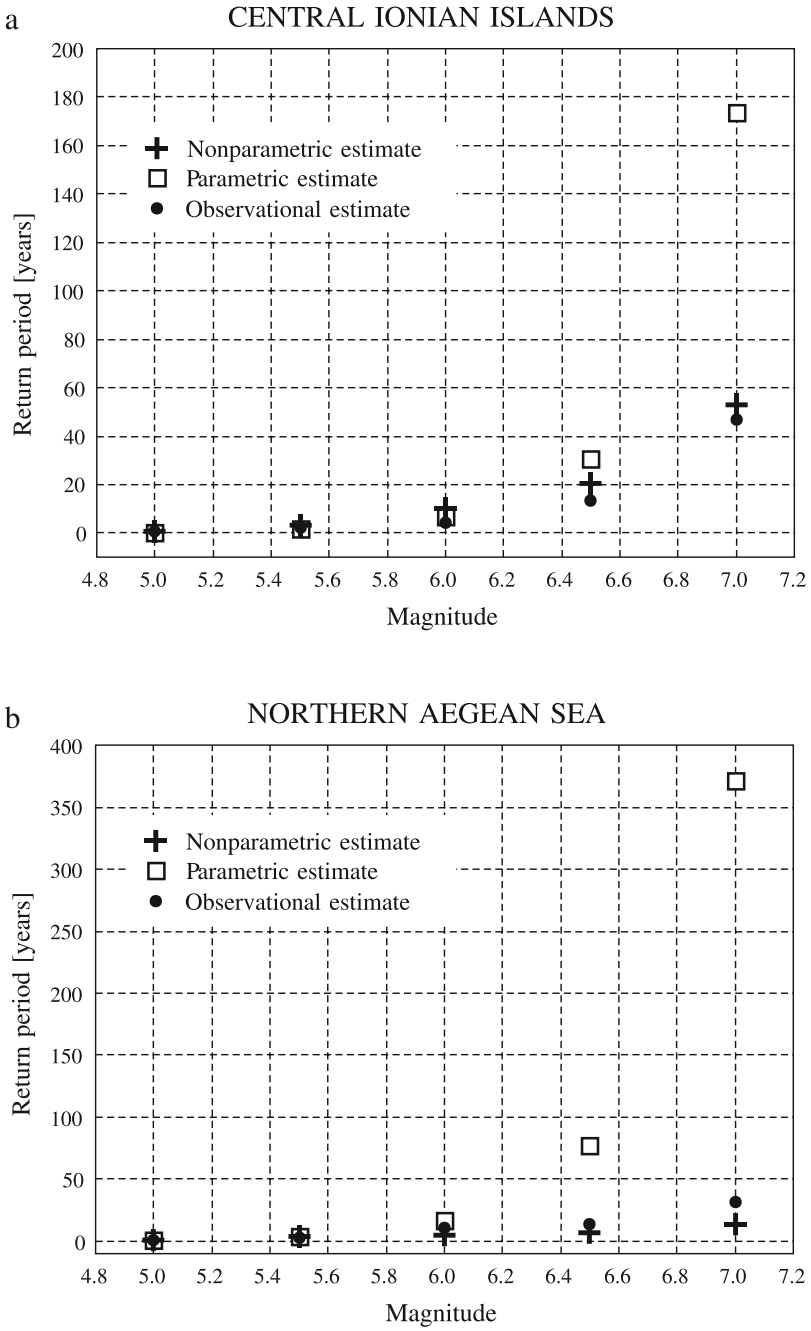

Figure 7. (a) Parametric estimates (squares), nonparametric estimates (crosses) and observational estimates (dots) of the mean return periods for central Ionian Islands area. (b) Same as in Figure 7a for the northern Aegean Sea area. (c) Same as in Figure 7a for the Thessalia area.

(1981–2001) has considerably overestimated the return periods of earthquakes of magnitude 6.5 and larger and the discrepancy is very large for the largest events. To the contrary, the nonparametric estimates obtained from the same data from 20 years are, for this magnitude range, close to the observational ones.

[39] For the Thessalia area, differences between return period estimates are not significant for magnitudes ≤ 5.5 (Figure 7c). For magnitudes 6.0 and 6.5, one can see the same effect as in the previous two cases, namely, larger recurrence intervals from the parametric approach compared to observational estimates. For magnitude 6.5, the parametric estimate of the return period is more than 9 times greater than the observational estimate (230 years and 24 years, respectively). However, for this magnitude the nonparametric estimate also considerably overestimates the return period compared to the observational value of the return period (89 and 24 years, respectively). Besides, the seismicity behavior in the Thessalia area is very peculiar. Strong events ($M \geq 6.2$) cluster both in time and space [*Papazachos et al.*, 1994]. This episodic occurrence was substantiated to take place three times in the last five centuries and interpreted in terms of stress interaction between neighboring fault segments [*Papadimitriou and*

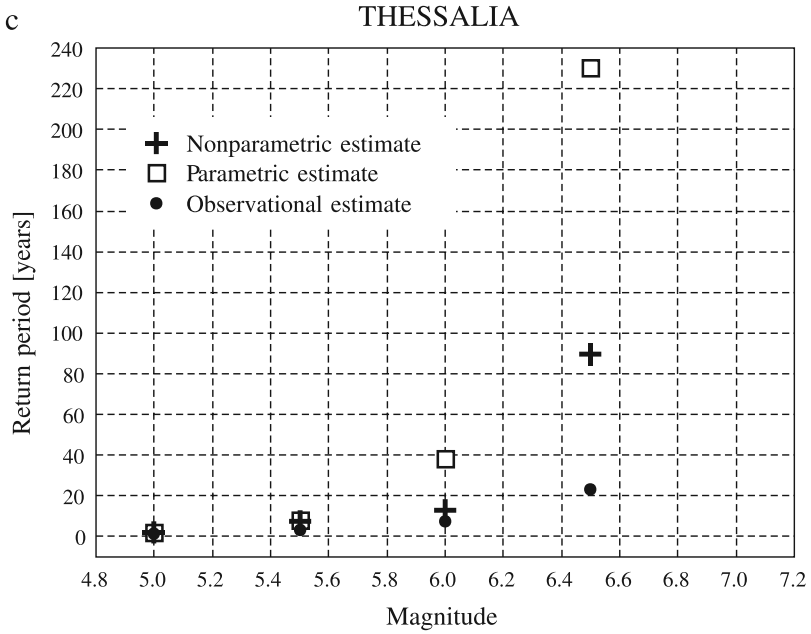

Figure 7. (continued)

Karakostas, 2003]. Therefore we reevaluated the observational return period estimates based on earthquakes that have occurred since the 16th century [*Papazachos and Papazachou*, 2003]. Our motive was to examine whether the mean return periods obtained from the occurrences of $M \geq 6.0$ events in the 20th century can serve as estimates of the long-term character of seismic activity in the Thessalia area or not, since the 20th century was an active period following a quiescent one. Parametric, nonparametric, 94-year observational and 460-year observational estimates of the mean return period for this area are provided in Table 3. A disagreement between the two observational estimates is seen, and can be attributed to increased seismic activity in the 20th century. The 460-year observational return periods agree, however, with the nonparametric estimates evaluated from the data for a 38 years period (1964–2001). Thus we conclude, from all the presented analyses of seismicity from the Thessalia area, that the nonparametric return period estimates the long-term character of the seismicity well, whereas the use of the classic log linear magnitude distribution model for hazard evaluation results in an overestimation of the mean return periods of large earthquakes. It is interesting that these last results were obtained for the study area for which the smoothed bootstrap test did not indicate a complex magnitude distribution, though, as stressed above, it has not indicated a simple distribution either.

8. Effect of Aftershock Removal

[40] The nonparametric, kernel estimation of magnitude distribution is a model-free, data-driven approach. Therefore, as addressed in section 7, the kernel estimator represents correctly all kinds of magnitude distributions: the single-component as well as the multicomponent distributions, regardless of the origin of particular probabilistic components of the final distribution. Thus the kernel estimate is expected to represent also correctly the mixture of a main event magnitude distribution and an aftershock magnitude distribution. This estimate will yield accurate estimates of the mean return periods concerning long recurrence intervals as long as both components of the long-term earthquake process: the main shock component and the aftershock component, are statistically represented in the data sample. In such a case declustering of the catalog prior to the hazard analysis would only unnecessarily reduce the sample size. For these reasons the data samples analyzed here were not declustered and comprised all earthquakes from the studied areas.

[41] It was, however, interesting to check whether the above expectations regarding the kernel estimation of magnitude were correct and study how much the obtained results, viz. a strong indication of the complexity of magnitude distribution and an accurate nonparametric estimation of long-term recurrence intervals, would be altered if aftershocks were removed from the sample data. For this purpose, aftershocks were removed from the CI40 sample from the central Ionian Islands area (Table 1) using the Reasenberg's declustering algorithm [*Reasenberg*, 1985]. The declustering procedure reduced the original sample from the initial 1256 data points to 595 values.

[42] The declustered sample was randomized according to the procedure presented in section 4 and used to test the null hypotheses on simplicity of the magnitude distribution, expressed by the presence of no more than one mode and

Table 3. Mean Return Period Estimates for the Thessalia Area[a]

	Mean Return Period Estimates, years			
M_c	Parametric (1964–2001)	Nonparametric (1964–2001)	Observational (1911–2004)	Observational (1544–2004)
6.0	38	13	8	16
6.5	230	89	24	87

[a]The nonparametric and parametric estimates were obtained from earthquake data for 1964–2001. The observational estimates were obtained from the data for 1911–2004 and for 1544–2004, respectively.

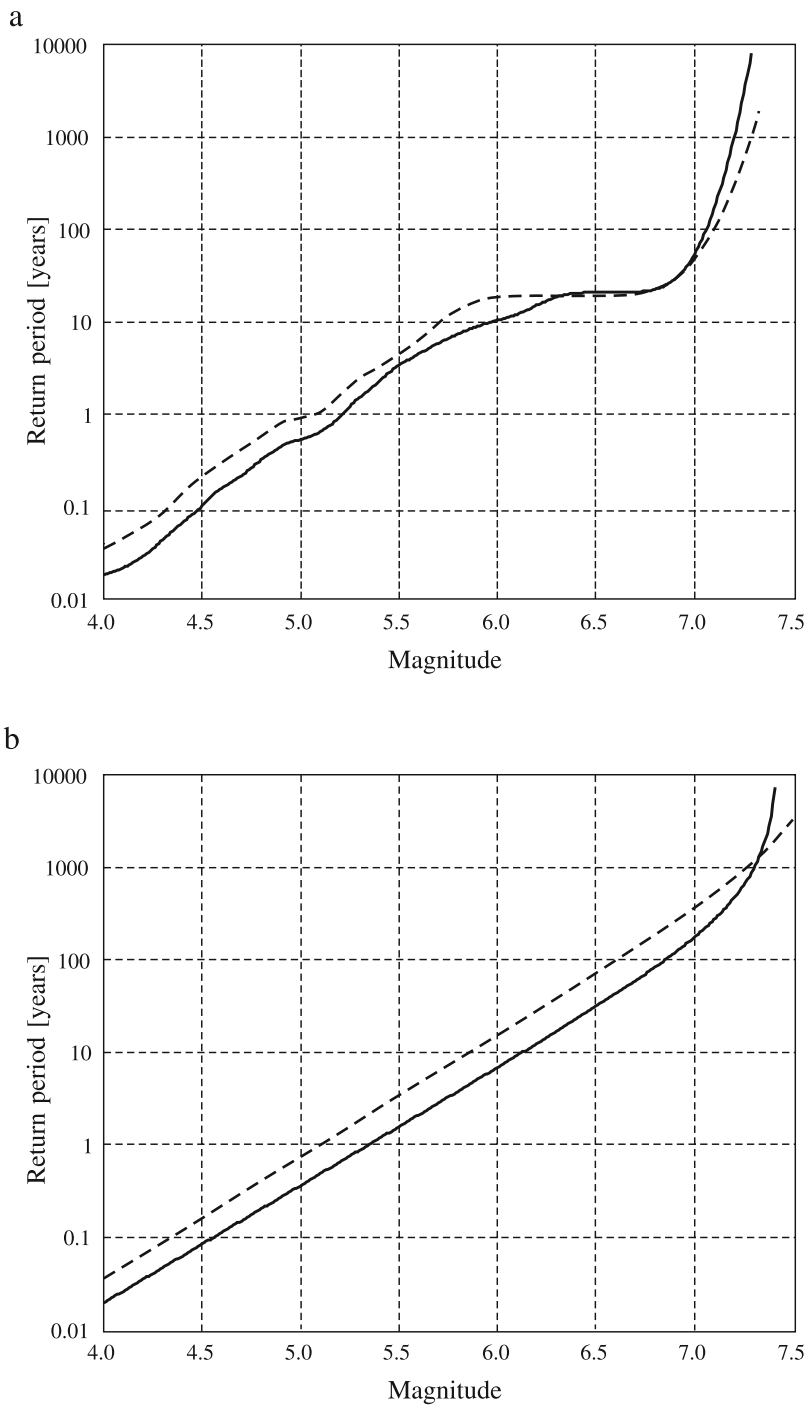

Figure 8. Estimates of the earthquake mean return period for the central Ionian Islands area obtained from the original data (continuous line) and the declustered data (dashed line) from 1981–2001. (a) Nonparametric estimates. (b) Parametric estimates.

one bump in the probability density (section 2.2). The calibrated results of the smoothed bootstrap test were: the significance of the null hypothesis H_o^1 (the probability density of magnitude is unimodal) $p = 0.05$ and the significance of the null hypothesis H_o^2 (the probability density of magnitude has one bump to the right of the mode) $p = 0.062$. These results signify slightly more strongly the complexity of the magnitude distribution of earthquake from central Ionian Islands area when compared to the results obtained from the original, not declustered CI40 sample, which are 0.069 and 0.08, respectively (Table 2). This effect, that traces of complexity of magnitude distribution become more distinct in samples from which aftershocks were removed, was also noticed by *Knopoff* [2000]. In our case it can be explained by the fact that the break in magnitude scaling for the central Ionian Islands earthquake data is located at a larger magnitude (M6.5–6.6, section 5). The removal of aftershocks, that were mostly of magnitudes from

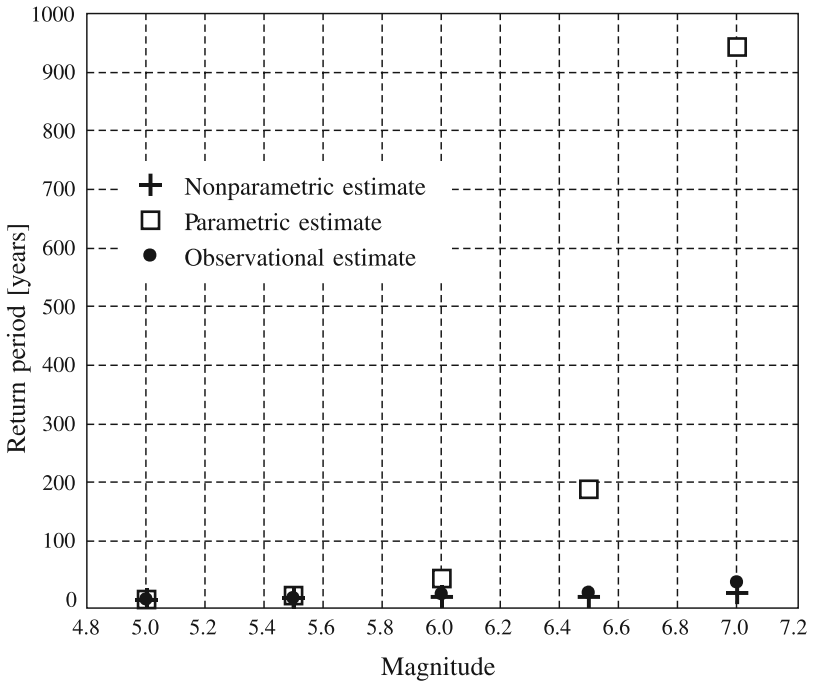

Figure 9. Parametric estimates (squares), nonparametric estimates (crosses) and observational estimates (dots) of the mean return periods obtained from declustered earthquake data for the central Ionian Islands area.

the lower part of the observed magnitude range, resulted in reducing the influence of weaker events on the empirical distribution of magnitude. In this way, the proportion in the sample of values associated with the second mode of the magnitude distribution increased.

[43] The nonparametric estimates of the mean return period from the original and the declustered central Ionian Islands earthquake data are compared in Figure 8a. The same comparison for the parametric estimates is shown in Figure 8b. In the magnitude range 4.0–6.3 the nonparametric return period estimate from the declustered sample is up to twice greater than the nonparametric estimate from the original sample (Figure 8a). This effect can be attributed to the fact that the removal of aftershocks reduced the overall sample size by some one half, determining in this way that the mean seismic activity of the main shocks was about twice less the mean activity when all events were taken into account. However, the shapes of $T(M_p)$ curves only slightly differ in this range. Not many aftershocks had magnitudes >6.0 therefore the declustering of data only enhanced the overrepresentation of stronger earthquakes compared to their number implied by the log linear distribution of magnitude. This gives rise to a flat part of the $T(M_p)$ curve from M6.0–6.8 and a slowing down of the rise of the return period with magnitude for magnitudes greater than 6.8.

[44] The differences between the parametric estimates of the return period obtained from the original and declustered samples (Figure 8b) result only from the decrease of the mean seismic activity. This is because the parametric estimate of magnitude CDF (equation (6)) is mostly controlled by events prevailing in the sample, and smaller events outnumbered the larger events even after the aftershocks were removed. The only significant change of the $T(M_p)$ curve is in the range of very strong events and is due to the fact that the estimate of the upper limit of magnitude distribution (equation (7)) from the declustered sample was greater than the same estimate from the not declustered data.

[45] The recurrence intervals estimated from declustered data for the period 1981–2001 were compared with the observational estimates from the catalog of 1911–2004. The observational estimates were evaluated in the same way as in section 7, that is, as a ratio 94 years to the number of occurrences of target events. This time, however, the catalog from 1911–2004 had to be also declustered before the observational estimates could be assessed. The obtained results are shown in Figure 9. For all considered magnitude values, the nonparametric estimate agrees with the observational estimate within the reasonable limits of statistical scatter. Thus, according to expectations, the removal of aftershocks had no effect on the accuracy of the nonparametric estimation of recurrence intervals. The disagreement between the parametric and observational estimates for magnitudes 6.5 and 7.0 is very large, larger than between the respective estimates obtained from the not declustered data.

9. Conclusions

[46] The complexity of the magnitude distributions underlying earthquake data from three different areas of Greece has been investigated by means of the smoothed bootstrap test for multimodality: the novel statistical method that does not require the making of any initial assumptions on the distribution model. The studied areas are among the most seismically active ones in the whole territory of Greece and are seismotectonically homogeneous, frequently accommodating strong ($M \geq 6.0$) events. The tested null hypotheses, that the magnitude density has no more than

one bump and that it has no more than one mode, were very general and covered all possible log linear or smoothly non–log linear distributions. Analysis of several data samples suggests the following:

[47] 1. In two out of the three studied cases, the magnitude distribution follows neither the log linear nor any smoothly non–log linear law but is more complex.

[48] 2. This complex magnitude distribution cannot be represented correctly by presently known, smoothly non–log linear parametric models. When such a model is applied, estimates of mean return periods dramatically disagree with earthquake recurrence observations over a longer time interval. The most significant differences occur for earthquakes having larger magnitudes, the most important cases for seismic hazard analysis.

[49] 3. The model-free approach with the kernel estimator of magnitude density ensures a satisfactory agreement between mean return period estimates and actual observations; in most cases, the agreement is very good: the ratio of the return period obtained from the probabilistic analysis to the return period estimated from long-term observations varies between 0.5 and 1.7. The presence of aftershocks in the data sample does not affect the accuracy of the recurrence interval estimates. On the basis of these results a model-free estimation of magnitude distribution is recommended for probabilistic seismic hazard analysis.

[50] **Acknowledgments.** This work was partially supported by the project 11.11.140.06 of the Faculty of Geology, Geophysics and Environmental Protection, AGH University of Science and Technology funded by the Ministry of Education and Science of Poland and the project of the General Secretariat of Research and Technology of Greece EPAN-M.4.3.6.1B. Geophysics Department contribution 673. We thank an anonymous Associate Editor, Margaret Boettcher, and the second anonymous referee for their valuable comments and suggestions.

References

Aki, K. (1965), Maximum likelihood estimate of b in the formula $\log N = a - bM$ and its confidence limits, *Bull. Earthquake Res. Inst. Univ. Tokyo*, *43*, 237–239.

Aki, K. (2000), Scale dependence in earthquake processes and seismogenic structures, *Pure Appl. Geophys.*, *157*, 2249–2258.

Bowman, A. W., P. Hall, and D. M. Titterington (1984), Cross-validation in non-parametric estimation of probabilities and probability densities, *Biometrika*, *71*, 341–351.

Cosentino, P., V. Ficarra, and D. Luzio (1977), Truncated exponential frequency-magnitude relationship in earthquake statistics, *Bull. Seismol. Soc. Am.*, *67*, 1615–1623.

Cox, D. R. (1966), Notes on the analysis of mixed frequency distributions, *Br. J. Math. Stat. Psychol.*, *19*, 39–47.

Davison, F. C., Jr., and C. H. Scholz (1985), Frequency-moment distribution of earthquakes in the Aleutian Arc: A test of the characteristic earthquake model, *Bull. Seismol. Soc. Am.*, *75*, 1349–1361.

Efron, B., and R. J. Tibshirani (1993), *An Introduction to the Bootstrap*, CRC Press, Boca Raton, Fla.

Jackson, D. D., and Y. Y. Kagan (1999), Testable earthquake forecasts for 1999, *Seismol. Res. Lett.*, *70*, 393–403.

Kagan, Y. Y. (1993), Statistics of characteristic earthquakes, *Bull. Seismol. Soc. Am.*, *83*, 7–24.

Kagan, Y. Y. (1996), Comment on "The Gutenberg–Richter or characteristic earthquake distribution, which is it?" by Steven G. Wesnousky, *Bull. Seismol. Soc. Am.*, *86*, 274–285.

Kagan, Y. Y. (1999), Universality of the seismic moment-frequency relation, *Pure Appl. Geophys.*, *155*, 537–573.

Kijko, A., and G. Graham (1998), Parametric-historic procedure for probabilistic seismic hazard analysis. part I: Estimation of maximum regional magnitude m_{max}, *Pure Appl. Geophys.*, *152*, 413–442.

Kijko, A., S. Lasocki, and G. Graham (2001), Nonparametric seismic hazard analysis in mines, *Pure Appl. Geophys.*, *158*, 1655–1676.

Klein, F. W., A. D. Frankel, C. S. Mueller, R. L. Wesson, and P. G. Okubo (2001), Seismic hazard in Hawaii: High rate of large earthquakes and probabilistic ground motion maps, *Bull. Seismol. Soc. Am.*, *91*, 479–498.

Knopoff, L. (2000), The magnitude distribution of declustered earthquakes in southern California, *Proc. Natl. Acad. Sci. U.S.A.*, *95*, 11,880–11,884.

Lasocki, S. (1993), Weibull distribution as a model for sequence of seismic events induced by mining, *Acta Geophys. Pol.*, *41*, 101–112.

Lasocki, S. (2001), Quantitative evidences of complexity of magnitude distribution in mining-induced seismicity: Implications for hazard evaluation, in *5th International Symposium on Rockbursts and Seismicity in Mines "Dynamic Rock Mass Response to Mining," Symp. Ser.*, vol. S27, edited by G. van Aswegen, R. J. Durrheim, and W. D. Ortlepp. pp. 543–550, S. Afr. Inst. of Min. and Metall., Johannesburg.

Lasocki, S. (2002), Testing complexity of magnitude distribution, paper presented at the XXVIII General Assembly of the European Seismological Commission, Genoa, Italy.

Lasocki, S., A. Kijko, and G. Graham (2000), Model-free seismic hazard estimation, in *Proceedings of the International Conference on Earthquake Hazard and Risk in the Mediterranean Region, EHRMR'99*, edited by H. Gokcekus, pp. 503–508, Educ. Found. of Near East Univ., Lefkosia, Cyprus.

Lasocki, S., A. Kijko, and G. Graham (2002), Model-free seismic hazard analysis, in *Seismogenic Process Monitoring*, edited by H. Ogasawara, T. Yanagidani, and M. Ando, pp. 327–339, A. A. Balkema, Brookfield, Vt.

Leonard, T., O. Papasouliotis, and I. G. Main (2001), A Poisson model for identifying characteristic size effects in frequency data: Application to frequency-size distributions for global earthquakes, "starquakes," and fault lengths, *J. Geophys. Res.*, *106*, 13,473–13,484.

Main, I. (2000), Apparent breaks in scaling in the earthquake cumulative frequency-magnitude distribution: Fact or artifact?, *Bull. Seismol. Soc. Am.*, *90*, 86–97.

McKenzie, D. P. (1970), The plate tectonics of the Mediterranean region, *Nature*, *226*, 239–243.

McKenzie, D. P. (1972), Active tectonics of the Mediterranean region, *Geophys. J.R. Astron. Soc.*, *30*, 109–185.

McKenzie, D. P. (1978), Active tectonics of the Alpine-Himalayan belt: The Aegean Sea and surrounding regions, *Geophys. J. R. Astron. Soc.*, *55*, 217–254.

Nalbant, S. S., A. Hubert, and G. C. P. King (1998), Stress coupling between earthquakes in northwest Turkey and the north Aegean Sea, *J. Geophys. Res.*, *103*, 24,469–24,486.

Orlecka-Sikora, B., and S. Lasocki (2005), Nonparametric characterization of mining induced seismic sources, in *Proceedings of the Sixth International Symposium on Rockburst and Seismicity in Mines 9–11 March 2005, Australia*, edited by Y. Potvin and M. Hudyma, pp. 555–560, Aust. Cent. for Geomech., Nedlands.

Pacheco, J. F., and L. R. Sykes (1992), Seismic moment catalog of large shallow earthquakes, 1900 to 1989, *Bull. Seismol. Soc. Am.*, *82*, 1306–1349.

Pacheco, J. F., C. H. Scholz, and L. R. Sykes (1992), Changes in frequency-size relationship from small to large earthquakes, *Nature*, *355*, 71–73.

Page, R. (1968), Aftershocks and microaftershocks, Bull, *Seismol. Soc. Am.*, *58*, 1131–1168.

Papadimitriou, E. E. (2002), Mode of strong earthquake recurrence in central Ionian Islands (Greece): Possible triggering due to Coulomb stress changes generated by the occurrence of previous strong shocks, *Bull. Seismol. Soc. Am.*, *92*, 3293–3308.

Papadimitriou, E. E., and V. G. Karakostas (2003), Episodic occurrence of strong ($M_w \geq 6.2$) earthquakes in Thessalia area (central Greece), *Earth Planet. Sci. Lett.*, *215*, 395–409.

Papadimitriou, E. E., and B. C. Papazachos (1985), Evidence for precursory seismicity patterns in the Ionian Islands (Greece), *Earthquake Predict. Res.*, *3*, 95–103.

Papadimitriou, E. E., and L. R. Sykes (2001), Evolution of the stress field in the northern Aegean Sea (Greece), *Geophys. J. Int.*, *146*, 747–759.

Papazachos, B. C., and P. E. Comninakis (1970), Geophysical features of the Greek island arc and eastern Mediterranean ridge, *C. R. Sceances Conf. Reunie Madrid 1969*, *16*, 74–75.

Papazachos, B. C., and P. E. Comninakis (1971), Geophysical and tectonic features of the Aegean Arc, *J. Geophys. Res.*, *76*, 8517–8533.

Papazachos, B. C., and C. Papazachou (2003), *The Earthquakes of Greece*, 317 pp., Ziti, Thessaloniki, Greece.

Papazachos, B. C., D. G. Panagiotopoulos, and G. F. Karakaisis (1994), Seismicity of northern Thessalia, paper presented at the 7th Congress of "Olympus in Eternity", Municipality of Elassona, Elassona, Greece, 1–9 Aug.

Papazachos, B. C., A. A. Kiratzi, and V. G. Karakostas (1997), Toward a homogeneous moment magnitude determination in Greece and surrounding area, *Bull. Seismol. Soc. Am.*, *87*, 474–483.

Papazachos, B. C., E. E. Papadimitriou, A. A. Kiratzi, C. B. Papazachos, and E. K. Louvari (1998), Fault plane solutions in the Aegean Sea and the surrounding area and their tectonic implications, *Boll. Geofis. Teor. Appl.*, *39*, 199–218.

Papazachos, B. C., P. E. Comninakis, G. F. Karakaisis, V. G. Karakostas, C. A. Papaioannou, C. B. Papazachos, and E. M. Scordilis (2005), A catalogue of earthquakes in Greece and surrounding area for the period 550BC–1999, report, Geophys. Lab., Univ. of Thessaloniki, Thessaloniki, Greece.

Papazachos, C. B., and A. A. Kiratzi (1996), A detailed study of the active crustal deformation in the Aegean and surrounding area, *Tectonophysics*, *253*, 129–153.

Pisarenko, V. F., and D. Sornette (2003), Characterization of the frequency of extreme earthquake events by the generalized Pareto distribution, *Pure Appl. Geophys.*, *160*, 2343–2364.

Reasenberg, P. (1985), Second-order moment of central California seismicity, 1969–1982, *J. Geophys. Res.*, *90*, 5479–5495.

Scholz, C. H. (2002), *The Mechanics of Earthquakes and Faulting*, 471 pp., Cambridge Univ. Press, New York.

Scordilis, E. M., G. F. Karakaisis, B. G. Karakostas, D. G. Panagiotopoulos, P. E. Comninakis, and B. C. Papazachos (1985), Evidence for transform faulting in the Ionian Sea: The Cephalonia Island earthquake sequence, *Pure Appl. Geophys.*, *123*, 388–397.

Silverman, B. W. (1986), *Density Estimation for Statistics and Data Analysis, Monogr.* CRC Press, Boca Raton, Fla.

Sornette, D., and A. Sornette (1999), General theory of the modified Gutenberg-Richter law for large seismic moments, *Bull. Seismol. Soc. Am.*, *89*, 1121–1130.

Sornette, D., L. Knopoff, Y. Y. Kagan, and C. Vanneste (1996), Rank-ordering statistics of extreme events: Application to the distribution of large earthquakes, *J. Geophys. Res.*, *101*, 13,883–13,893.

Stirling, M. W., S. G. Wesnousky, and K. Shimazaki (1996), Fault trace complexity, cumulative slip, and the shape of the magnitude-frequency distribution for strike-slip faults: A global survey, *Geophys. J. Int.*, *124*, 833–868.

Stock, C., and E. G. C. Smith (2000), Evidence for different scaling of earthquake source parameters for large earthquakes depending on faulting mechanism, *Geophys. J. Int.*, *143*, 157–162.

Triep, E. G., and L. R. Sykes (1997), Frequency of occurrence of moderate to great earthquakes in intracontinental regions: Implications for changes in stress, earthquake prediction, and hazards assessments, *J. Geophys. Res.*, *102*, 9923–9948.

Utsu, T. (1999), Representation and analysis of the earthquake size distribution: A historical review and some new approaches, *Pure Appl. Geophys.*, *155*, 509–535.

Wesnousky, S. G., C. H. Scholz, K. Shimazaki, and T. Matsuda (1983), Earthquake frequency distribution and the mechanics of faulting, *J. Geophys. Res.*, *88*, 9331–9340.

S. Lasocki, Faculty of Geology, Geophysics and Environmental Protection, AGH University of Science and Technology, Krakow, Poland. (lasocki@geol.agh.edu.pl)

E. E. Papadimitriou, Geophysics Department, School of Geology, Aristotle University of Thessaloniki, GR-54124, Thessaloniki, Greece. (ritsa@geo.auth.gr)